Estimation of Grid Frequency in Disturbed Converter-Based Power Systems by PLL State Variable Feedback

Nico Goldschmidt, Horst Schulte

University of Applied Sciences (HTW) Berlin,
Department of Engineering I, Control Engineering Group,
Wilhelminenhofstr. 75A, 12459 Berlin, Germany,
Email: {nico.goldschmidt,schulte}@htw-berlin.de

Abstract: Fast real-time estimation of the grid frequency is essential for stable operation of renewable converter-based sources in future power systems. Therefore this paper presents a new phase-locked loop for the estimation of time-dependent frequencies in unbalanced power systems with harmonics. The proposed frequency estimation method consists of two signal processing steps: In the first step, a least mean square estimator reconstructs the fundamental sinusoidal signal from the measured three-phase grid voltage and splits it into positive, negative and zero sequence components. In the second step, the resulting first harmonic three-phase positive sequence is converted into the synchronous reference frame in the form of a phase-locked loop using a state feedback controller scheme to reconstruct the current grid frequency. Here the controller output is equivalent to the signal to be reconstructed. The feedback controller design is based on linear matrix inequalities where the requirements are explicitly considered. The capability of proposed state feedback phase-locked loop is demonstrated by full scaled electro magnetic transient simulations.

Keywords: Estimation algorithms, Phase-locked loop, Power system control, Renewable energy systems, Convex optimisation

1. INTRODUCTION

Continuous increase of renewable energy power plants in power systems requires their integration as active control units for grid stabilization and forming. In addition, the reduction of conventional energy producers causes more disturbances and parts of harmonics in the electrical power systems, which lead to a higher variation of the frequency and voltage. However, the precise detection of fundamental symmetrical components is crucial for a reliable network supporting operation of renewable converter based sources even in severely disturbed areas of operation.

A proven method to estimate the current first harmonic phase angle and frequency of the electrical grid is the phase-locked loop algorithm (PLL). In the following an overview of different types of PLL based methods is given. In order to ensure nearly ideal conditions in power grids without distortion or unbalance, the synchronous reference frame PLL in combination with an classic proportional integral (PI) controller is the most appropriate and widely used method, see Chung (2000) and Rolim et al. (2006). However, under unbalanced grid conditions, the negative sequence components cause a second harmonic of the voltage vector. For robust operation, the feedback dynamics must be limited significantly with the result that the PLL response speed would become very slow. Therefore, in recent years several improved schemes based on modified PLL techniques have been developed which remove the unbalanced components and high-order harmonics using

suitable pre-processing. A distinction can be made between two pre-processing methods:

T1 Symmetrical components are first formed from the disturbed signal and then particular harmonics are decoupled from the used signal

T2 Desired harmonics are filtered out at the beginning and the symmetrical components are formed afterwards

The decoupled double synchronous reference frame PLL (dd-SRF-PLL) proposed by Rodriguez et al. (2007) and the decoupled multi synchronous reference frame PLL (md-SRF-PLL), see Xu et al. (2009) belongs to the Type 1 (T1) procedure. The disadvantage is that only a few components can be decoupled, whereby the effort increases proportionally. With Type 2 (T2) methods, on the other hand, the desired basic signal is filtered out at the beginning. In Zhang et al. (2013) and Pradhan et al. (2005) a least mean square filter is used for this task.

The approach presented in this paper based on the Type 2 pre-processing method. However, for the final frequency reconstruction a novel state feedback controller scheme with Linear Matrix Inequality (LMI) based design is proposed. This paper is organized as follows: First, in Section 2 the modelling of the phase-locked loop, with synchronous reference frame approach is presented. In Section 3, the state-feedback design for robust frequency and phase estimation is proposed. It is shown, that stability is guaranteed by employing a Lyapunov function which is formulated by

LMIs. All necessary design steps are presented in detail. Subject of consideration in Section 4 is the separation of measured three phases in symmetrical components using a least mean square estimator formulation taken from Zhang et al. (2013). It follows the presentation of simulation results, the discussion and conclusion in Section 6 and Section 7.

1.1 Nomenclature

For a better understanding, the nomenclature in Tab.1 provides an overview of the used symbols.

Table 1. Overview of symbols

Symbol	Definition
$[\cdot]_{abc}$	three phase system
$[\cdot]_{dq}$	synchronous reference frame
$[\cdot]_c$	constant, equilibrium point
$\tilde{[\cdot]}$	extended
$[\cdot]_{red}$	reduced
Δ	difference
$\widehat{[\cdot]}$	estimated value
$[\cdot]^{\perp}$	orthogonal
$[\cdot]^{(1)}$	first harmonic
$[\cdot]^{(n)}$	n-th harmonic
$[\cdot]^{+,-,0}$	symmetrical components

2. SIGNAL DESCRIPTION AND TRANSFORMATIONS FOR PLL DESIGN

The complete signal chain for the phase estimation introduced here is illustrated in Figure 3. It contains various transformations and appropriate signal descriptions of the three-phase system.

First, the formal basis of PLL modelling is provided by the synchronous voltage reference frame in d-q coordinates. The corresponding coordinators $\mathbf{v}_{dq} = (v_d \; v_q)^T$ are calculated from the symmetric components of the three phase system $\mathbf{v}_{abc} = (v_a \; v_b \; v_c)^T$ by the Clark and the Park transformation

$$\begin{pmatrix} v_d \\ v_q \end{pmatrix} = \frac{2}{3} \underbrace{\begin{pmatrix} \cos(\widehat{\varphi}) & \cos(\widehat{\varphi} - \frac{2}{3}\pi) & \cos(\widehat{\varphi} + \frac{2}{3}\pi) \\ -\sin(\widehat{\varphi}) & -\sin(\widehat{\varphi} - \frac{2}{3}\pi) & -\sin(\widehat{\varphi} + \frac{2}{3}\pi) \end{pmatrix}}_{\mathbf{T}_{dq}(\widehat{\varphi})} \begin{pmatrix} v_a \\ v_b \\ v_c \end{pmatrix} , \quad (1)$$

where $\widehat{\varphi}$ denotes the estimated phase angle. It should be noted that a synchronous coordinate system can be formed with the Clark and the Park transformation (1) if the configuration of the three-phase system is symmetric. However, an arbitrarily unbalanced three-phase system is given by the superposition of three symmetric components

$$\begin{aligned} v_a &= v_a^+ + v_a^- + v_a^0 , \\ v_b &= v_b^+ + v_b^- + v_b^0 , \\ v_c &= v_c^+ + v_c^- + v_c^0 \end{aligned} \quad (2)$$

with the positive sequence components v_x^+, negative sequence components v_x^-, and zero sequence components v_x^0

with $x = a, b, c$. In particular, the symmetrical components are defined as follows

$$\begin{aligned} v_a^+ &= -V^+ \sin(\varphi^+) , \\ v_b^+ &= -V^+ \sin(\varphi^+ - \tfrac{2}{3}\pi) , \\ v_c^+ &= -V^+ \sin(\varphi^+ + \tfrac{2}{3}\pi) , \end{aligned}$$

$$\begin{aligned} v_a^- &= -V^- \sin(\varphi^- + \varphi_n) , \\ v_b^- &= -V^- \sin(\varphi^- + \varphi_n + \tfrac{2}{3}\pi) , \\ v_c^- &= -V^- \sin(\varphi^- + \varphi_n - \tfrac{2}{3}\pi) , \end{aligned} \quad (3)$$

with

$$\varphi_n = |\varphi^+| - |\varphi^-| , \quad \varphi^- = -\varphi^+ , \quad (4)$$

where V^+, V^- denote the magnitudes and φ^+, φ^- denote the phase angles of the positive and negative component. Note that the zero components are not taken into account because the park transformation yields a zero vector. Thus (1) can be applied to a unbalanced system by transforming the single symmetrical components $\mathbf{v}_{abc}^+$ and $\mathbf{v}_{abc}^-$ individually. By substituting $\mathbf{v}_{abc} = (v_a \; v_b \; v_c)^T$ in (3) by the symmetric components (2) follows with (1) and the addition theorem

$$\begin{aligned} v_d &= \underbrace{-V^+ \sin(\Delta\widehat{\varphi}^+)}_{v_d^+} + \underbrace{V^- \sin(\Delta\widehat{\varphi}^+ - \varphi_n)}_{v_d^-} \\ v_q &= \underbrace{V^+ \cos(\Delta\widehat{\varphi}^+)}_{v_q^+} - \underbrace{V^- \cos(\Delta\widehat{\varphi}^+ - \varphi_n)}_{v_q^-} , \end{aligned} \quad (5)$$

where $\Delta\widehat{\varphi}^+$ denotes the difference between the reconstructed and true phase angle

$$\Delta\widehat{\varphi}^+ = \varphi^+ - \widehat{\varphi} \quad (6)$$

The derivation of (5) leads to

$$\begin{aligned} \dot{v}_d^+ &= -\Delta\widehat{\omega}^+ V^+ \cos(\Delta\widehat{\varphi}^+) \\ \dot{v}_q^+ &= -\Delta\widehat{\omega}^+ V^+ \sin(\Delta\widehat{\varphi}^+) \\ \dot{v}_d^- &= (\Delta\widehat{\omega}^+ - \omega_n) V^- \cos(\Delta\widehat{\varphi}^+ - \varphi_n) \\ \dot{v}_q^- &= (\Delta\widehat{\omega}^+ - \omega_n) V^- \sin(\Delta\widehat{\varphi}^+ - \varphi_n) \end{aligned} \quad (7)$$

with

$$\Delta\widehat{\omega}^+ = \Delta\dot{\widehat{\varphi}}^+ , \quad \omega_n = \dot{\varphi}_n >> 0 \quad . \quad (8)$$

By inserting (5) into (7) it is possible to simplified the differential equation system. In summary, this results in

$$\begin{pmatrix} \dot{v}_d^+ \\ \dot{v}_q^+ \\ \dot{v}_d^- \\ \dot{v}_q^- \end{pmatrix} = \begin{pmatrix} -\Delta\widehat{\omega}^+ v_q^+ \\ \Delta\widehat{\omega}^+ v_d^+ \\ -\Delta\widehat{\omega}^+ v_q^- \\ \Delta\widehat{\omega}^+ v_d^- \end{pmatrix} . \quad (9)$$

For the model-oriented control design it is necessary to transform (9) in the state space form:

$$\dot{\mathbf{x}} = \mathbf{f}(\mathbf{x}, u) = \begin{pmatrix} 0 & -u & 0 & 0 \\ u & 0 & 0 & 0 \\ 0 & 0 & 0 & -u \\ 0 & 0 & u & 0 \end{pmatrix} \mathbf{x} = \mathbf{A}(u)\mathbf{x} \quad (10)$$

with the state vector

$$\mathbf{x} = (\mathbf{x}^+ \; \mathbf{x}^-)^T = (v_d^+ \; v_q^+ \; v_d^- \; v_q^-)^T , \quad (11)$$

the output vector $\mathbf{y}$ and the input scalar u

$$\mathbf{y} = \mathbf{x} , \quad u = \Delta\widehat{\omega}^+ . \quad (12)$$

It is interesting to note that the deduced non linear state space model (10) has no affine input u but appears as a variable parameter in the system matrix $\mathbf{A}(u)$.

3. STATE SPACE FEEDBACK DESIGN WITH POLE SPECIFICATION

In this section a systematic LMI-based design according to Chilali and Gahinet (1996), Arzelier et al. (1993), Gutman and Jury (1981) is presented for further use in the entire PLL design. In contrast to classical PI controller design the approach enables a pole placement in a desired region in the complex plane by LMI-constraints.

3.1 Closed-loop Pole Assignment by LMI-constraints

Based on the linearised uncertain system of (10)

$$\Delta \dot{\mathbf{x}} = \mathbf{A}_c \, \Delta \mathbf{x} + \mathbf{b}_c \, \Delta u \qquad (13)$$

with the equilibrium point

$$\mathbf{x}_c = [1, 0, 0, 0]^T , \; u_c = 0 , \qquad (14)$$

$\mathbf{A}_c$ as the system matrix and $\mathbf{b}_c$ as the input vector, the objective is to find a state variable feedback

$$\Delta u = -\mathbf{k}^T \Delta \mathbf{x} \qquad (15)$$

such that the closed-loop eigenvalues of $\left(\mathbf{A} - \mathbf{b}\mathbf{k}^T \right)$ are in $S(\alpha_{min}, \alpha_{max})$. The so defined pole region $S(\alpha_{min}, \alpha_{max})$ is shown in Fig. 1. The constraint of the closed loop eigen-
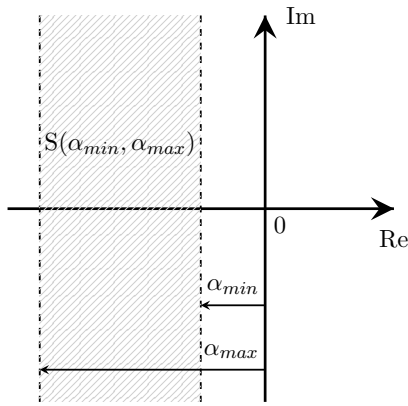

Fig. 1. Pole region S $(\alpha_{min}, \alpha_{max})$

values within a predefined region $S(\alpha_{min}, \alpha_{max})$ guarantees a desired performance specified by an maximum overshoot, the frequency range of the damped oscillations, rise time, and settling time as shown in Chilali and Gahinet (1996). However, it is assumed that there is a feasible solution to the LMI condition (17).

The system (13) controlled by state variable feedback (15) is exponentially stable in respective to the defined region $S(\alpha_{min}, \alpha_{max})$ if there exists a Lyapunov function

$$\mathbf{V}(\Delta \mathbf{x}) = \Delta \mathbf{x}^T \mathbf{P} \Delta \mathbf{x}, \; \mathbf{P} > 0 \qquad (16)$$

with $\mathbf{P} = \mathbf{P}^T \in \mathbb{R}^{n \times n}$ and $\mathbf{X} = \mathbf{P}^{-1}$ that fulfils

$$-2\alpha_{max}\mathbf{X} < \mathbf{A}_c\mathbf{X} + \mathbf{X}\mathbf{A}_c^T - \mathbf{b}_c\mathbf{m} - \mathbf{m}^T\mathbf{b}_c^T < -2\alpha_{min}\mathbf{X} \qquad (17)$$

with $\alpha_{max} > \alpha_{min} > 0$ where $\mathbf{m} \in \mathbb{R}^{1 \times n}$. As described in Chilali and Gahinet (1996) and Arzelier et al. (1993) this results in the state feedback matrix

$$\mathbf{k}^T = \mathbf{m}\,\mathbf{X}^{-1} \qquad (18)$$

for (15).

3.2 Extension of Closed-loop Design for Setpoint Sequences

After the short description of the LMI-based pole region design, it will be extended to a setpoint control for $\mathbf{y}_{ref} \neq \mathbf{0}$. In order to be able to guarantee the stability of the closed loop, the integrator eigenvalues must be controllable. According to the criterion of Hautus, the r integral eigenvalues $\lambda = 0$ can be controlled, if and only if the condition

$$\begin{pmatrix} \mathbf{A}_c & \mathbf{0} & | & \mathbf{b}_c \\ \mathbf{c}_c^T & 0 & | & d_c \end{pmatrix} = n + r \qquad (19)$$

is fulfilled. For the estimation of the actual angular frequency value with the synchronous reference frame approach the exact regulation of the positive q component to ZERO is necessary, so the output matrix $\mathbf{c}_c$ is defined by

$$\mathbf{c}_c^T = \begin{pmatrix} 0 & 1 & 0 & 0 \end{pmatrix} . \qquad (20)$$

Taking into account the output matrix $\mathbf{c}_c$, we get the extended system and input matrix

$$\tilde{\mathbf{A}}_c = \begin{pmatrix} \mathbf{A}_c & \mathbf{0} \\ -\mathbf{c}_c^T & \mathbf{0} \end{pmatrix} \in \mathbb{R}^{(n+1) \times (n+1)} , \qquad (21)$$

$$\tilde{\mathbf{b}}_c = \begin{pmatrix} \mathbf{b} \\ 0 \end{pmatrix} \in \mathbb{R}^{(n+1) \times m} \qquad (22)$$

The setpoint control law can then be specified for the extended system with the input

$$\Delta \tilde{u} = - \begin{pmatrix} \mathbf{k}_x & -k_I \end{pmatrix} \begin{pmatrix} \Delta \mathbf{x} \\ \Delta r \end{pmatrix} \qquad (23)$$

and

$$\Delta r = \int \Delta e \, d\tau \; , \; \Delta e = \Delta y_{ref} - \mathbf{c}_c^T \Delta \mathbf{x} \qquad (24)$$

as follows

$$\Delta \tilde{u} = -\mathbf{k}_x^T \Delta \mathbf{x} + k_I \int \Delta e \, d\tau \; . \qquad (25)$$

For the sake of clarity, previous results are summarized in Fig. 2. The block diagram illustrates the I-augmented feedback control structure including the transformation of a three phase system into a synchronous reference frame for positive and negative sequences.

4. LEAST MEAN SQUARE ESTIMATOR

The following section is taken from Zhang et al. (2013). As written in Zhang et al. (2013) an unbalanced and distorted three phase system can be represented as

$$\begin{aligned} v_a &= \sum_{n=1}^{N} V_a^n \sin(n\omega t + \phi_a^n) \\ v_b &= \sum_{n=1}^{N} V_b^n \sin(n\omega t + \phi_b^n) \qquad (26) \\ v_c &= \sum_{n=1}^{N} V_c^n \sin(n\omega t + \phi_c^n) \end{aligned}$$

with

$$t = k \, T_s \; , \quad k \in \mathbb{N}^+ \qquad (27)$$

where $V_{a,b,c}$ are the magnitudes, ω is the fundamental circular frequency, T_s is the sampling interval, k is the sampling instant and $\phi_{a,b,c}$ are the initial phase angles depending on the n-th harmonic component. Further,
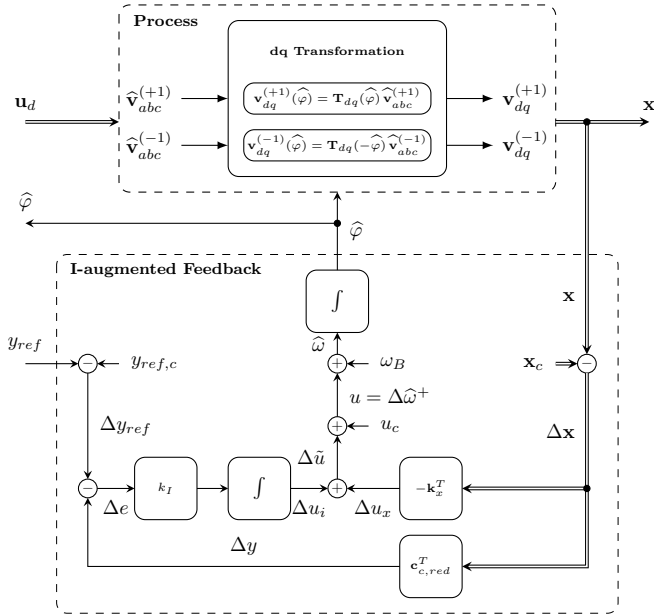
Fig. 2. Block diagram of the I-augmented feedback control

following the calculation in Zhang et al. (2013) with the substitution

$$\omega k T_s + \phi_a^1 = \varphi_a + \theta_a \ , \tag{28}$$

where φ_a denotes the estimated phase angle and θ_a the estimated error, and in combination with the simplification of (26) related to the fundamental oscillation, we get the following equations

$$
\begin{aligned}
v_a &= V_a^1 \cos(\theta_a) \sin(\varphi_a) + V_a^1 \sin(\theta_a) \cos(\varphi_a) \\
v_b &= V_b^1 \cos(\theta_b) \sin(\varphi_a) + V_b^1 \sin(\theta_b) \cos(\varphi_a) \\
v_c &= V_c^1 \cos(\theta_c) \sin(\varphi_a) + V_c^1 \sin(\theta_c) \cos(\varphi_a)
\end{aligned} \tag{29}
$$

with

$$\theta_b = \theta_a + \phi_b^1 - \phi_a^1 , \quad \theta_c = \theta_a + \phi_c^1 - \phi_a^1 \ . \tag{30}$$

In preparation for the implementation of a linear adaptive filter approach (29) can be expressed as a regression function

$$\widehat{\mathbf{Y}} = \mathbf{W}\mathbf{X} \tag{31}$$

with the estimated output vector of the fundamental grid voltage

$$\widehat{\mathbf{Y}} = (\widehat{v}_a \ \widehat{v}_b \ \widehat{v}_c)^T \ , \tag{32}$$

the matrix of weighting coefficients

$$
\mathbf{W} = \begin{pmatrix}
V_a^1 \cos(\theta_a) & V_a^1 \sin(\theta_a) \\
V_b^1 \cos(\theta_b) & V_b^1 \sin(\theta_b) \\
V_c^1 \cos(\theta_c) & V_c^1 \sin(\theta_c)
\end{pmatrix} \tag{33}
$$

and the input vector

$$\mathbf{X} = (\sin(\varphi_a) \ \cos(\varphi_a))^T \ . \tag{34}$$

For the required angle of the input vector, the reconstructed angle of the PLL (see Fig. 2) is used

$$\varphi_a = \widehat{\varphi} \quad . \tag{35}$$

The Least Mean Square algorithm applied here relies on a relatively simple and robust adaptive filter technique (Pradhan et al. (2005)). The weighting matrix $\mathbf{W}(k+1)$ per iteration step is calculated with

$$\mathbf{W}(k+1) = \mathbf{W}(k) + \mu \, \mathbf{e}(k) \, \mathbf{X}^T(k) \left[\mathbf{X}(k)\mathbf{X}^T(k) \right]^{-1} \ . \tag{36}$$

The choice of the adaptation parameter μ (Zhang et al. (2013), Pradhan et al. (2005)) determines how fast the estimates follows changes in the data by minimum mean-square error $\mathbf{e}(k)$

$$\mathbf{e}(k) = (e_a \ e_b \ e_c)^T = (u_a - \widehat{u}_a, \ u_b - \widehat{u}_b, \ u_c - \widehat{u}_c)^T \ . \tag{37}$$

If $\widehat{\mathbf{Y}}$ is reconstructed by the estimated weight matrix (36) and the orthogonal $\widehat{\mathbf{Y}}^\perp$ is known

$$\widehat{\mathbf{Y}}^\perp = \mathbf{W}' \mathbf{X} \tag{38}$$

with

$$\widehat{\mathbf{Y}}^\perp = \left(\widehat{v}_a^\perp \ \widehat{v}_b^\perp \ \widehat{v}_c^\perp \right)^T \tag{39}$$

and

$$
\mathbf{W}' = \begin{pmatrix}
w_{11} & -w_{12} \\
w_{21} & -w_{22} \\
w_{31} & -w_{32}
\end{pmatrix} \tag{40}
$$

then the division into three symmetric components according to Zhang et al. (2013) based on the instantanous theory is feasible. Using (2) and split the components into the real and imaginary part, we get the matrices

$$
\begin{aligned}
\widehat{\mathbf{Y}}^+ &= \mathbf{T}_1 \widehat{\mathbf{Y}} + \mathbf{T}_2 \widehat{\mathbf{Y}}^\perp , \\
\widehat{\mathbf{Y}}^- &= \mathbf{T}_1 \widehat{\mathbf{Y}} - \mathbf{T}_2 \widehat{\mathbf{Y}}^\perp , \\
\widehat{\mathbf{Y}}^0 &= \mathbf{T}_3 \widehat{\mathbf{Y}} ,
\end{aligned} \tag{41}
$$

that are related to the three symmetric components with

$$
\mathbf{T}_1 = \frac{1}{3} \begin{pmatrix}
1 & -0,5 & -0,5 \\
-0,5 & 1 & -0,5 \\
-0,5 & -0,5 & 1
\end{pmatrix} ,
$$

$$
\mathbf{T}_2 = \frac{1}{2\sqrt{3}} \begin{pmatrix}
0 & 1 & -1 \\
-1 & 0 & 1 \\
1 & -1 & 0
\end{pmatrix} , \ \mathbf{T}_3 = \frac{1}{3} \begin{pmatrix}
1 & 1 & 1 \\
1 & 1 & 1 \\
1 & 1 & 1
\end{pmatrix} \tag{42}
$$

obtained from the complex phase shift operators

$$
\begin{aligned}
\beta &= e^{j\frac{2}{3}\pi} = -\frac{1}{2} + \frac{\sqrt{3}}{2}j , \\
\beta^2 &= e^{j\frac{4}{3}\pi} = -\frac{1}{2} - \frac{\sqrt{3}}{2}j , \\
\beta^3 &= e^{j\frac{6}{3}\pi} = 1 .
\end{aligned}
$$

As result, the first harmonic can be separated from the grid disturbances with (36) and (39) and then decomposed into the symmetric components with (41) and (42). These inherit the inputs of the I-augmented feedback PLL, see Fig. (2). An overview of the adaptive filter involving all previous operations is illustrated in Fig. 3.

5. SIMULATION RESULTS

The following study is a part of the research project Windkraftwerk/Wind Power Plant (funding reference number: 0325935B) which has the more general objective to investigate the behaviour of converter-controlled electrical grids and to design robust control strategies for future
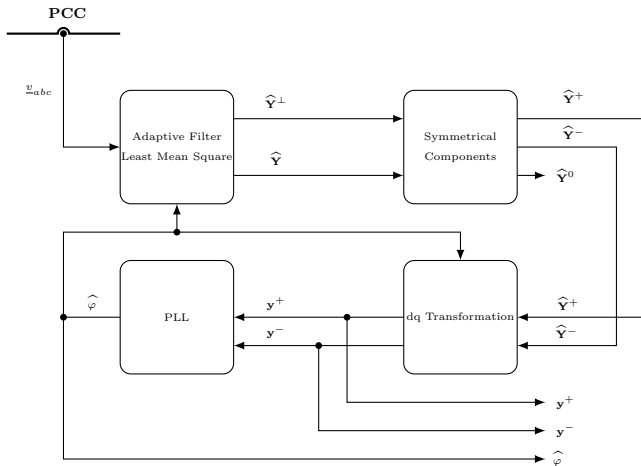
Fig. 3. Block diagram of the adaptive filter and control structure

converter systems, especially for grid integration of wind turbines. Part of the project was to develop a test bench with a total of eight freely configurable inverters each with a rated active power of $P_N = 11$kW and a switching frequency $f_S = 3900$Hz, see Kisser et al. (2017). The designed control structures can be upload employing the MATLAB/Simulink auto-code generation capabilities. A part of the future work is the experimental validation of the presented approaches at the test bed system. In this paper simulation results are presented.

The reference parameters of the inverter to be examined are

$$v_{AC,ref} = \sqrt{2} \cdot 230\,V \ , \ v_{DC,ref} = 640\,V \ ,$$
$$i_{ref} = \sqrt{2} \cdot 16\,A \quad , \ \omega_{G,ref} = 2\pi 50\,\tfrac{1}{s} \ . \tag{43}$$

As a preliminary stage of an experimental validation, the proposed concepts are tested in a full-scaled simulation environment developed in MATLAB/Simulink-Simscape, which reproduces the behaviour of a real system up to the PWM switching level. The performance of the novel I-augmented feedback PLL with adaptive filter is demonstrated in this simulation environment and compared with the dd-SRF-PLL presented in Rodriguez et al. (2007). For the simulation a fixed-step discrete solver is used at $t_{step} = \frac{1}{f_S} = 256\mu$s. The step size of the adaptive filter is set to $\mu = 0.128$. This is the best compromise between the simulation speed and accuracy. The fundamental frequency is 50 Hz and corresponds to 1 p.u. The dd-SRF-PLL was implemented in the test bed system as part of a master thesis at the HTW Berlin.

5.1 Case 1: Distorted Unbalanced System (DUS)

The first test case deals with a combination of measurement disturbance and a two phase short circuit of the first and second phase without ground fault. The nominal disturbance is based on random noise signals of $\pm 10\%$ p.u. voltage level added to each phase of the undisturbed three phase system. The total simulation time is $T = 1$ s. The short circuit starts $t = 0,\overline{3}s$ and ends at $t = 0.\overline{6}$s, with approx 50% residual voltage, illustrated in Fig. 4.
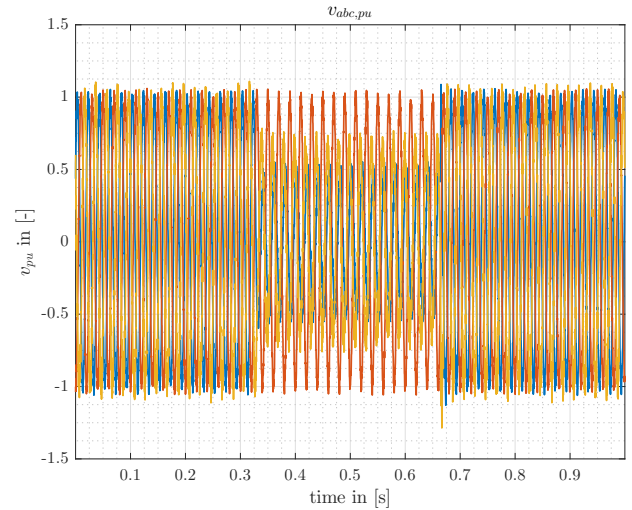

Fig. 4. Original three phase system under random distorted and unbalanced conditions

Fig. 5 shows the estimated frequency under distorted unbalanced conditions. The yellow dashed line corresponds to the actual frequency value. The red line shows the estimated frequency of the I-augmented feedback PLL with adaptive filter and the blue line corresponds to the estimated frequency of dd-SRF-PLL scheme. The
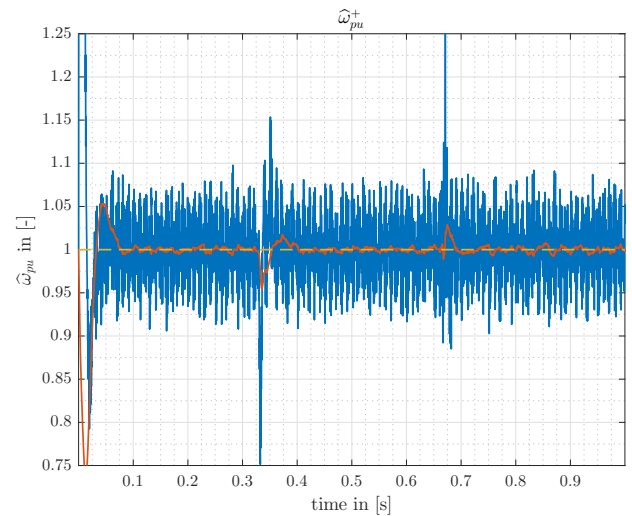

Fig. 5. Reconstructed relative frequency under random distorted and unbalanced conditions

voltage related to d-q coordinates separated into positive and negative sequence is illustrated in Fig. 6. The red line corresponds to the I-augmented feedback PLL with adaptive filter and the blue line shows the behaviour of the dd-SRF-PLL.

5.2 Case 2: Frequency Variation

The second test case contains a frequency variation inspired by Rueda-Escobedo et al. (2019). The behaviour is illustrated in Fig. 7. The total simulation time is $T = 60$s. The yellow dashed line corresponds to the reference value. The red line shows the estimated frequency value of the I-augmented feedback PLL with adaptive filter and the
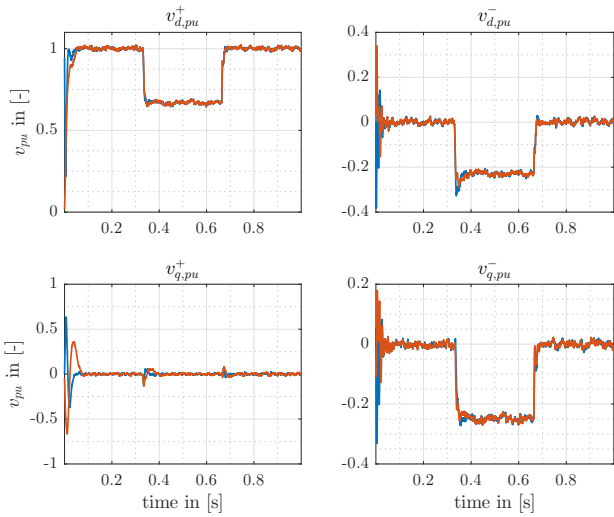
Fig. 6. Positive and negative components in d-q frame under random distorted and unbalanced conditions

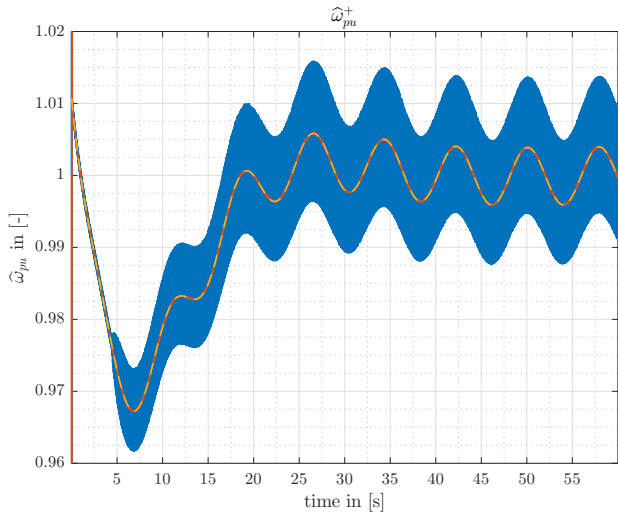blue line corresponds with the estimated frequency value of dd-SRF-PLL.

Fig. 7. Reconstructed relative frequency in frequency variation

5.3 Case 3: DUS with Harmonics

The last test case inspired by Zhang et al. (2013) based on the distorted unbalanced system of the first test case extended by 10% of the 5th and 6% of the 7th harmonic in the three phase system. The simulation time is also $1s$. The three phase system is illustrated in Fig. 8. Fig. 9 shows the estimated frequency under distorted unbalanced conditions. The yellow dashed line corresponds to the actual frequency value. The red line shows the estimated frequency value of the I-augmented feedback PLL with adaptive filter and the blue line corresponds with the estimated frequency value of dd-SRF-PLL. The voltage related to d-q coordinates separated into positive and negative sequence is illustrated in Fig. 10. The red line corresponds to the I-augmented feedback PLL with adaptive filter and the blue line is the behaviour of the dd-SRF-PLL.
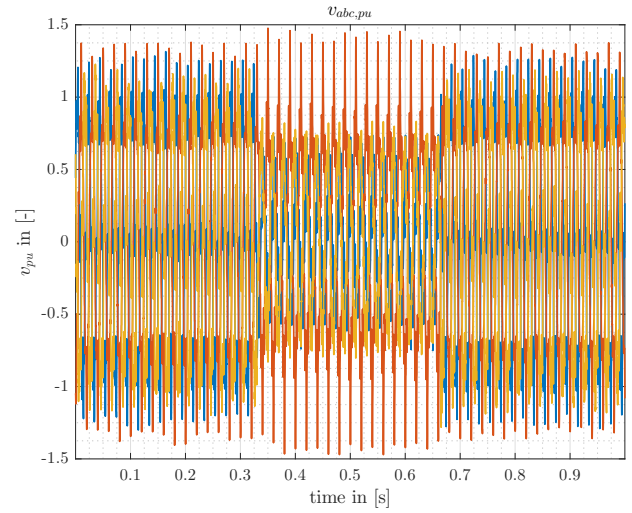

Fig. 8. Original three phase system with 5th and 7th harmonic and unbalanced conditions
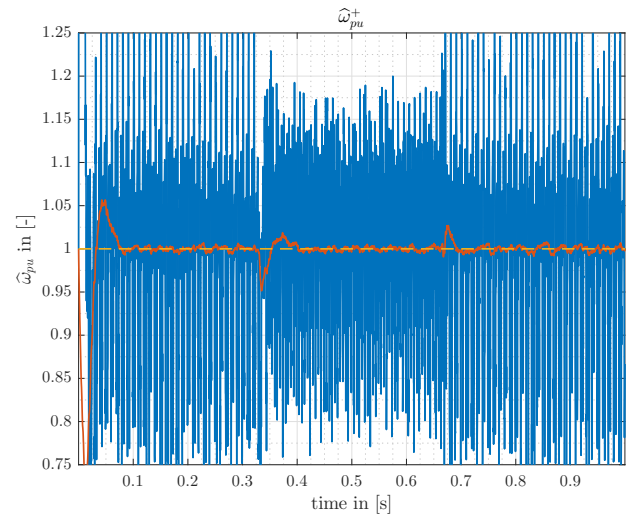

Fig. 9. Reconstructed relative frequency with 5th and 7th harmonic and unbalanced conditions
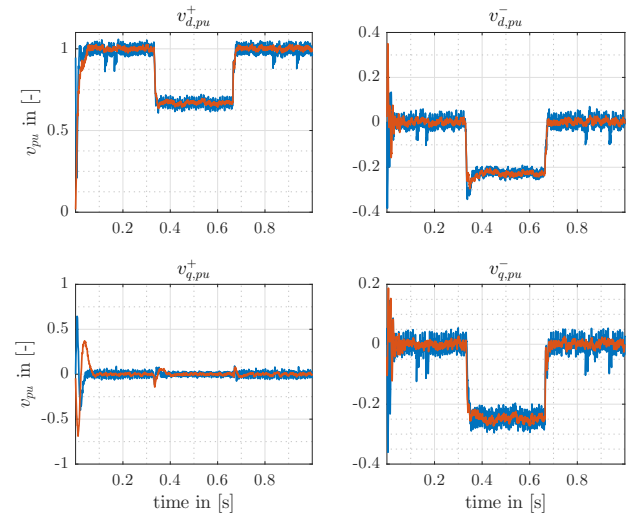

Fig. 10. Positive and negative components in d-q frame with 5th and 7th harmonic and unbalanced conditions

6. DISCUSSION

The results of the dd-SRF-PLL and the I-augmented feedback PLL with adaptive filter will compared and discussed. Note that the discussion based on the fact of increasing number of converter-based power supplies in the future. This caused to an increase in electrical grid pollution, especially in the form of harmonics, as well as a higher frequency variation. This is taken into account in the considered test cases.

As already shown in Zhang et al. (2013), both approaches have a short settling time and also a stable and robust behaviour with low interference under the conditions of a full-scaled simulation environment. With increasing disturbance and higher frequency variations it can be seen that the dd-SRF-PLL gets difficulties with the reconstruction of the grid angle frequency. The structural advantages of the filter can be seen here, that cancels all other frequencies with the exception of the fundamental harmonics of the incoming system and simultaneously transforms the filtered three-phase into its symmetrical components. In particular, the increase in harmonics clearly shows the limits of the dd-SRF-PLL. The performance can be improved by further decoupling elements per harmonic (method is denoted by dm-SRF-PLL), but the degree of complexity and necessary computing performance increase (see Xu et al. (2009)). In contrast, a reliable estimation of the grid angle frequency can be achieved with the proposed I-augmented feedback PLL even with strong increasing disturbance and higher frequency variations.

7. CONCLUSION

In this paper a method for estimating the grid frequency in a disturbed three-phase system was presented. The method is based on an already published adaptive filter (Zhang et al. (2013)) and a novel scheme with a state feedback controller that replaces the existing PI controller structure. The relevant problem formulation and the LMI-based design was presented in detail and simulation results compared to existing methods were discussed. In a subsequent study, the procedure is implemented in the HTW test bench and undergoes further system tests are carried out, in particular for various faults in power systems.

REFERENCES

Arzelier, D., Bernussou, J., and Garcia, G. (1993). Pole assignment of linear uncertain systems in a sector via a Lyapunov-type approach. *IEEE Transactions on Automatic Control*, 38(7), 1128–1132. doi:10.1109/9.231470.

Chilali, M. and Gahinet, P. (1996). H∞ design with pole placement constraints: An LMI approach. *IEEE Transactions on Automatic Control*, 41(3), 358–367. doi:10.1109/9.486637.

Chung, S.K. (2000). A phase tracking system for three phase utility interface inverters. *IEEE Transactions on Power Electronics*, 15(3), 431–438.

Gutman, S. and Jury, E. (1981). A general theory for matrix root-clustering in subregions of the complex plane. *IEEE Transactions on Automatic Control*, 26(4), 853–863. doi:10.1109/TAC.1981.1102764.

Kisser, A., Engel, M., Rezai, L., Andrejewski, M., Fortmann, J., and Schulte, H. (2017). A Test-bed System for Validation of Ancillary Services of Wind Power Plants under Realisitic Conditions. In *Proceedings of 16th Wind Integration Workshop*. Berlin.

Pradhan, A.K., Routray, A., and Basak, A. (2005). Power System Frequency Estimation Using Least Mean Square Technique. *IEEE Transactions on Power Delivery*, 20(3), 1812–1816. doi:10.1109/TPWRD.2004.843453.

Rodriguez, P., Pou, J., Bergas, J., Candela, J.I., Burgos, R.P., and Boroyevich, D. (2007). Decoupled Double Synchronous Reference Frame PLL for Power Converters Control. *IEEE Transactions on Power Electronics*, 22(2), 584–592. doi:10.1109/TPEL.2006.890000.

Rolim, L.B., da Costa Jr, D.R., and Aredes, M. (2006). Analysis and software implementation of a robust synchronizing PLL circuit based on the pq theory. *IEEE Transactions on Power Electronics*, 53(6), 1919–1926.

Rueda-Escobedo, J.G., Moreno, J.A., and Schiffer, J. (2019). Finite-Time Estimation of Time-Varying Frequency Signals in Low-Inertia Power Systems. In *2019 18th European Control Conference (ECC)*, 2108–2114. doi:10.23919/ECC.2019.8795926.

Xu, L., Han, Y., Khan, M., Zhou, L., Yao, G., Chen, C., and Pan, J. (2009). A novel control strategy for dynamic voltage restorer using decoupled multiple reference frame PLL (DMRF-PLL). *WSEAS Transactions on Systems*, 8, 261–277.

Zhang, X.G., Duan, D.K., Chen, J.M., Liu, Y.C., and Xu, D.G. (2013). A robust synchronization method for grid sequence extraction. *Przeglad Elektrotechniczny*, 89, 101–109.